Effect of processing history on shrinkage stress in axially oriented poly(ethylene terephthalate) fibres and films

V. B. Gupta*, J. Radhakrishnan and S. K. Sett†
Department of Textile Technology, Indian Institute of Technology, New Delhi 110016, India
(Received 27 April 1993; revised 4 November 1993)

Axially oriented poly(ethylene terephthalate) fibres and films with widely differing processing histories were prepared by varying the spinning speed in the case of fibres and the speed, temperature, medium and extent of drawing for both fibres and films. The samples were held at constant length and heated to temperatures between 60 and 220°C with simultaneous recording of their thermomechanical response for up to 20 s. Samples produced at low speeds developed low shrinkage stress, which decayed with time. On the other hand, samples produced at relatively higher speeds developed higher shrinkage stress, which showed little relaxation with time. The structural basis of these results is discussed, and the roles played by processing parameters highlighted.

(Keywords: shrinkage stress; poly(ethylene terephthalate); orientation)

INTRODUCTION

Drawn polymeric fibres and films shrink at elevated temperatures, as the extended molecules tend towards a coiled conformation because of entropic considerations. If the samples are held at constant length and not allowed to shrink, the entropic forces of contracting segments are balanced by the reaction of external constraints. Then the whole molecular network is under tension, which hinders further shrinkage and increases the possibility of relaxation processes becoming operative, like breaking of the physical links of the stressed network leading to intermolecular slipping[1]. The temperature and time dependences of shrinkage tension have been studied for polycarbonate (PC), poly(ethylene terephthalate) (PET) and polyethylene (PE) by Trznadel and coworkers[2–5], for nylon-6 by Dennis and Buchanan[6], and for PET by Ward and coworkers[7–10], Heuvel *et al.*[11], Hearle and Mukhopadhyay[12], Desai and Abhiraman[13] and Batra[14]. A recent review[15] shows that these studies have resulted in enhancing our comprehension of the effects of molecular orientation and the nature of the network and to a lesser extent of crystallinity and recrystallization on shrinkage stress. However, the roles played by the process variables and structure in the thermomechanical and stress-optical behaviour of PET fibres and films, in particular in the generation and relaxation of shrinkage stress, are not clearly understood[7,15].

In the present investigation, axially oriented PET fibres and films with widely differing processing histories were prepared and characterized for time and temperature dependence of shrinkage stress. The emphasis was on the time dependence of shrinkage stress up to 15 s, when the sample was surrounded by an air oven set to raise the sample temperature to 100 and 220°C, respectively. The results of shrinkage studies on these samples have already been reported[16].

EXPERIMENTAL

Preparation of starting samples

Fibres. Three kinds of fibres were made. Some physical characteristics of the starting samples are summarized in *Table 1*.

(i) Monofilament: Single filaments of 130 denier were spun from fibre-grade PET chips in a laboratory spinning unit. The filaments were quenched in water at around 5°C, 25 cm below the spinneret, before being wound at 10 m min^{-1}.

(ii) Low-oriented yarn (LOY): Multifilament PET yarns 165/36/0, i.e. of 165 denier, 36 filaments and zero twist, were produced on an industrial unit at 1000 m min^{-1} by Orkay Polyester, Bombay, India.

(iii) Partially oriented yarn (POY): Multifilament PET yarns 126/36/0, i.e. of 126 denier, 36 filaments and

Table 1 Some physical characteristics of undrawn samples

Sample	Winding speed (m min^{-1})	Birefringence, Δn	Density (g cm^{-3})	X-ray crystallinity (%)
Film	10	ND[a]	1.336	ND
Monofilament	10	ND	1.339	ND
Multifilament yarn (LOY)	1000	0.007	1.342	ND
Multifilament yarn (POY)	3000	0.038	1.349	2

[a] ND = Not detectable

* To whom correspondence should be addressed
† Present address: College of Textile Technology, Serampore 712201, India

0032-3861/94/12/2560–08

Table 2 Sample designation and drawing conditions

Sample No.	Starting sample	Drawing conditions: Temp. (°C)	Medium (stages)	Draw ratio	Equivalent draw ratio	Draw rate (min^{-1})
1	Film	70	Water (2)	2.1 (1.46, 1.46)	2.1	1–3
2	Film	70	Water (2)	3.1 (1.46, 2.06)	3.1	1–3
3	Film	70	Water (2)	4.16 (2.08, 2.00)	4.16	1–3
4	Monofilament	70	Water (2)	4.16 (2.08, 2.00)	4.16	3
5	LOY	90	Air (1)	3.4	4.1	20
6	POY	90	Air (1)	1.62	4.16	13

zero twist, were produced on an industrial unit at 3000 m min^{-1} by Modipon Ltd, Modinagar, India.

Film. An 80 μm thick, 30 mm wide film was melt cast from fibre-grade PET chips and wound on chilled rollers at 10 m min^{-1} by Garware Polyester, Aurangabad, India. Characteristics are shown in *Table 1.*

Uniaxial drawing of the samples

The spun fibres and cast film were drawn in air and/or in water under conditions described later. The drawing conditions for samples on which detailed studies have been made are summarized in *Table 2.* The sample number indicated in the table will be used hereafter to refer to the respective drawn samples.

Drawing of filaments in air at 90°C. The spun multifilament yarns (LOY and POY) were uniaxially stretched on a laboratory drawing machine by passing them over a heater plate of length 25 cm at a temperature of 90°C to various extents up to a total draw ratio of 5 at strain rates between 2 and 20 min^{-1}. For estimating the total draw ratio, the residual draw was taken[17] as 1.2 for LOY and as 2.6 for POY.

Drawing of film and filaments in water at 70°C. The PET film was drawn to different draw ratios in water at 70°C in two stages at strain rates between 1 and 3 min^{-1}. The monofilament was drawn to a draw ratio close to 4.2 under similar conditions.

Measurement of drawing stress

The tension in the running filament or film as it emerged from the heater plate or water bath and before it was taken up by the draw rollers was measured with the help of a Rothschild R 1192 electronic tensiometer.

Density crystallinity

The densities of the samples were measured using a density gradient column prepared from n-heptane and carbon tetrachloride. The mass crystalline fraction was estimated from the measured density (ρ) using the following expression:

$$\text{Mass crystalline fraction} = \frac{\rho_c}{\rho}\left(\frac{\rho-\rho_a}{\rho_c-\rho_a}\right) \quad (1)$$

where ρ_c and ρ_a are the crystalline and amorphous densities respectively; they were taken to be $\rho_c = 1.455$ g cm^{-3} and $\rho_a = 1.333$ g cm^{-3} (ref. 18).

Birefringence

A polarizing microscope fitted with a tilting compensator was used to measure the sample birefringence. The thickness of the film was measured with the help of a precision digital micrometer, while the diameter of the fibre was measured with the help of an eyepiece micrometer.

X-ray diffraction studies

The X-ray diffraction studies were made to measure crystallinity and crystallite orientation using methods described elsewhere[19].

Amorphous birefringence and amorphous orientation factor

The total measured birefringence, Δn, was assumed to be the sum of the specific birefringence values of the crystalline (Δn_c) and amorphous (Δn_a) phases[19,20] with appropriate weighting:

$$\Delta n = \beta \Delta n_c + (1-\beta)\Delta n_a \quad (2)$$

where β is the degree of crystallinity. In expanded form equation (2) may be written as:

$$\Delta n = \beta f_c \Delta n_{c0} + (1-\beta) f_a \Delta n_{a0} \quad (3)$$

where Δn_{c0} and Δn_{a0} are the intrinsic crystalline and amorphous birefringences, respectively, and were taken as $\Delta n_{c0} = 0.22$ and $\Delta n_{a0} = 0.275$[21]. The amorphous orientation factor (f_a) of the samples could then be estimated from equation (3) after inserting the values of measured birefringence (Δn), crystallinity (β) and crystallite orientation factor (f_c).

Boiling water shrinkage

The percentage shrinkage, $S(\%)$, of different samples was measured in boiling water at 100°C. Samples were kept for 5 min in boiling water and then removed and allowed to come to room temperature. Percentage shrinkage was obtained using the following expression

$$S(\%) = \frac{(L_0 - L_s)}{L_0} \times 100 \quad (4)$$

where L_0 = initial length and L_s = length after shrinkage.

Shrinkage force

Multifilament yarn in the form of coiled loop or film strips of 2 mm width and 5 cm length was clamped with little pretension between two grips, one of which was connected to an Instron load cell. The sample was then quickly heated by raising a cylindrical heating device

preheated to a desired temperature, so that it surrounded the sample completely. The shrinkage force that was generated as a result of the heating of the sample was recorded on the Instron recorder as a function of time. The maximum value of the stress was taken as the peak shrinkage stress at that particular temperature.

RESULTS AND DISCUSSION

Shrinkage stress data at 100 and 220°C

The results of shrinkage stress measurements for samples 1 to 6 (*Table 2*) at temperatures of 100 and 220°C and for times up to 15 s are presented in *Figures 1a* and *1b* respectively. In all cases the retractive force increases initially and then (a) either tends to stabilize or stabilizes into a plateau region, or (b) decays, slowly in some cases and rapidly in others.

The sample takes a finite time to reach the desired temperature after being surrounded by the heating device, as shown in *Figure 1c*. As expected, the rate of heating up to 100°C is higher when the sample is surrounded by the heating device set to give a temperature of 220°C.

The shrinkage stress characteristics for the samples studied show considerable differences, the following being particularly noteworthy: (i) The stress builds up much more rapidly at 220°C than at 100°C. (ii) The absolute values of maximum stress (σ_{max}) generated for different samples show significant differences; in particular, samples 1 to 4 produced at low speeds generate relatively low stresses. (iii) For each of the six samples studied, the σ_{max} values at 100 and 220°C are quite close. (iv) Samples 5 and 6, which have been prepared at relatively high speeds, do not show any detectable relaxation of stress, while in the remaining samples, which have been produced at low speeds, stress relaxes slowly at 100°C and rapidly at 220°C.

Structural data

To gain an insight into the structural basis for these differences, some structural characteristics of the samples before and after heat treatment at 100 and 220°C were determined and are listed in *Table 3*. The large differences between crystallinity, as estimated from X-ray diffraction and density for the control samples 3 and 4, are noteworthy and have been attributed[16] to the paracrystalline or distorted crystal structure of these samples, which are highly oriented structures with compact packing of the molecules but poor longitudinal and transverse order. A large increase in X-ray crystallinity occurs when these samples are heat treated at 100°C. The birefringence changes on heat treatment are not large; there is a small decrease for samples of intermediate draw ratios, while for the high-draw-ratio samples, the birefringence either remains constant or shows a slight increase. Since contributions to birefringence are made up of contributions from the crystalline and amorphous phases, these observed changes, though small, contain useful information about

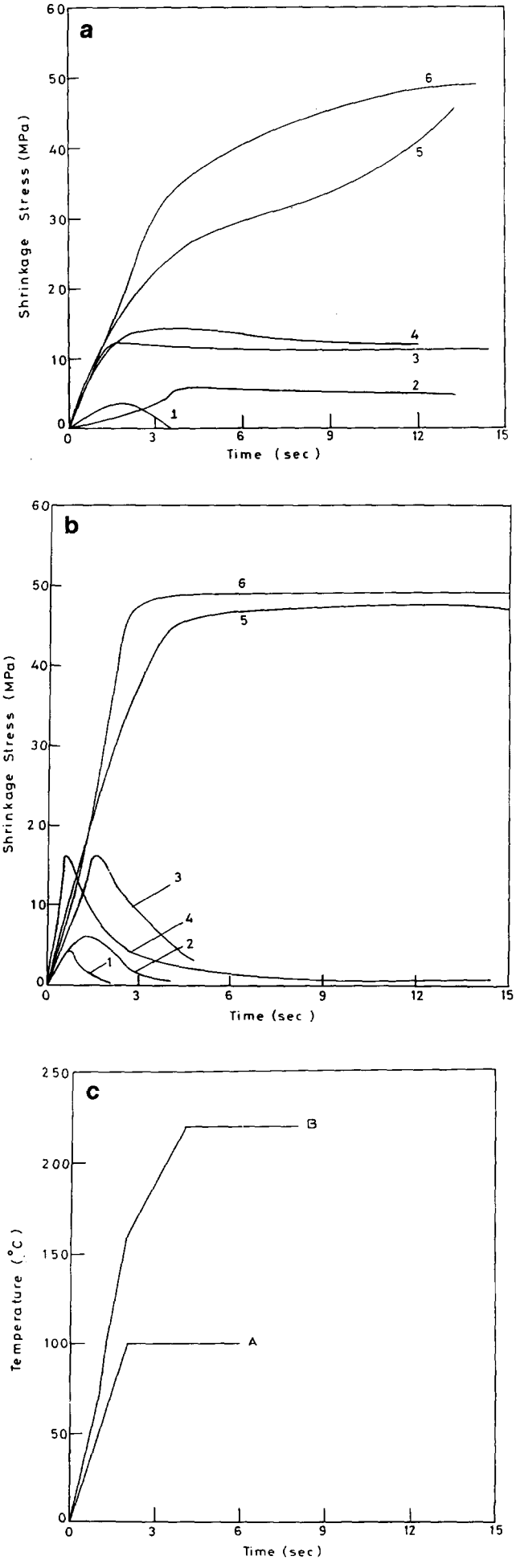

Figure 1 (a) Shrinkage stress at 100°C as a function of time (sample numbers as in *Table 2*). (b) Shrinkage stress at 220°C as a function of time (sample numbers as in *Table 2*). (c) Temperature–time relationship for the sample surrounded by the heater set to bring the sample to (A) 100°C and (B) 220°C

Table 3 Structural data for various samples

Sample No.[a]	Birefringence, Δn			Degree of crystallinity: X-ray			Degree of crystallinity: Density			Orientation factor	
		After heat treatment			After heat treatment			After heat treatment		Control	
	Control	100°C	220°C	Control	100°C	220°C	Control	100°C	220°C	f_c	f_a
1	0.034	0.033	0.030	0.033	0.08	0.20	0.066	0.12	0.36	0.89	0.104
2	0.090	0.088	0.090	0.050	0.10	0.32	0.11	0.19	0.38	0.91	0.313
3	0.176	0.175	0.176	0.08	0.37	0.55	0.24	0.32	0.65	0.90	0.630
4	0.188	0.188	0.186	0.07	0.36	0.54	0.24	0.33	0.56	0.91	0.680
5	0.210	0.210	0.226	0.27	0.35	0.52	0.25	0.35	0.52	0.94	0.797
6	0.171	0.171	0.187	0.28	0.34	0.56	0.25	0.36	0.53	0.92	0.578

[a] As in *Table 2*

the orientation of the amorphous phase, as will become clear from the analysis presented later.

The structural basis of generation and relaxation of shrinkage stress in these samples will be discussed after considering the results of other experimental studies on some of the samples under investigation.

Frozen-in axial stress

Isothermal drawing results in deformation, which consists of an irreversible component and a frozen viscoelastic component; the latter relates to the axial stress exerted in drawing[22]. Thus for the as-drawn samples the limiting values of σ_{max} would be expected to be equal in absolute value to the frozen-in axial stress. The measured values of σ_{max} at 100 and 220°C for some of the samples studied are plotted as a function of the measured drawing stress in *Figure 2*, and it is interesting to note that the shrinkage stress is always less than the drawing stress; this observation is consistent with the findings of other authors[1]. This may be because the molecular network undergoes transformation owing to the presence of highly organized structural elements and significant internal stresses in the sample, thus making it difficult for the sample to achieve its initial dimensions even after it is heated well above the melting point[1].

Another noteworthy observation is that the absolute value of the drawing stress is low for samples 1 to 4, which have been produced at low rates, while it is high for samples 5 and 6, which have been produced at relatively higher rates. This is apparently because (i) a very slow rate of drawing allows chain relaxation and disentanglement, thus lowering the frozen-in axial stress, (ii) the precursors for samples 5 and 6 had significant preorientation whereas the precursors for the other samples were isotropic, and (iii) samples 5 and 6 develop significant crystallinity on drawing.

Temperature dependence of shrinkage stress

The shrinkage stress studies for samples 3 and 5 were made over a wide temperature range, namely from 40 to 220°C. The plots of σ_{max} vs. heat treatment temperature for these two samples are presented in *Figure 3* and show two noteworthy features.

(i) Initially σ_{max} increases with increase in temperature and then stabilizes at a certain plateau, which extends above T_g. As expected, the shrinkage stress is low at low temperatures. As the temperature increases beyond T_g,

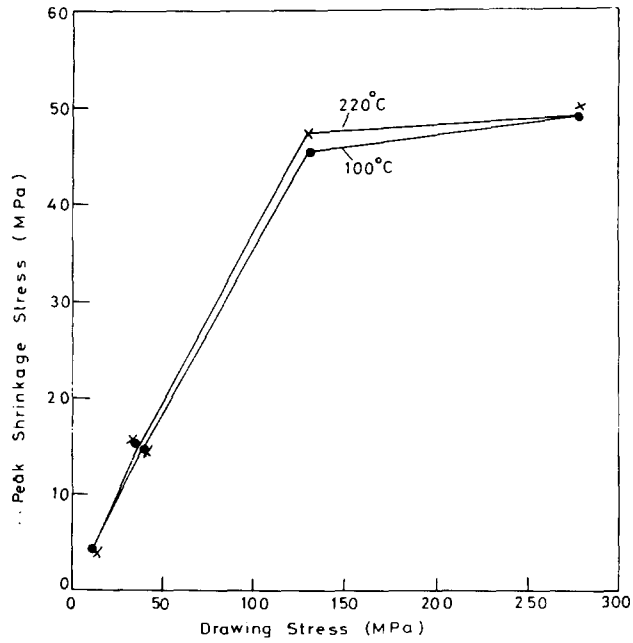

Figure 2 Peak shrinkage stress at 100°C (●) and 220°C (×) vs. drawing stress

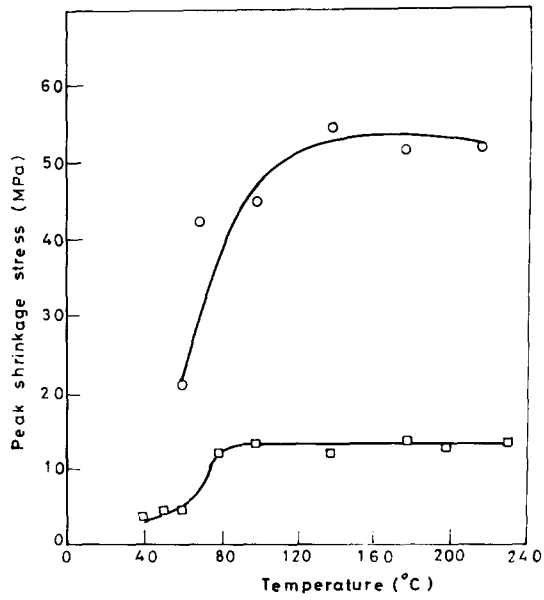

Figure 3 Plot of σ_{max} vs. heat treatment temperature for samples 3 (□) and 5 (○)

the entropic mechanism would start contributing to the shrinkage stress. With further increase in temperature, crystallization can occur and growth of crystallites can stabilize the oriented state, making relaxation of the stress difficult. The stress is likely to fall to zero when the crystalline substance melts.

(ii) Sample 5 develops much higher stresses than sample 3 and, as discussed earlier, this may be attributed to the presence of higher frozen-in axial stress present in the former.

The effect of draw ratio on shrinkage stress

The maximum shrinkage stress generated at 100 and 220°C in the film drawn to different draw ratios in water and in air is shown in *Figures 4a* and *4b* and in the POY sample drawn in air to different draw ratios in *Figure 4c*. The following four observations may be made:

(i) σ_{max} increases with increase in draw ratio. This is an expected result and brings out the importance of molecular orientation; the higher the orientation, the higher is the stress.

(ii) There is no significant effect of the heat treatment temperature on the magnitude of σ_{max}. As shown in *Figures 1a* and *1b* and also in *Figure 3*, this was also the case for a number of other samples and therefore this observation deserves further discussion.

The possible reasons for the magnitudes of σ_{max} at 100 and 220°C being very close may be sought in the generally accepted view[6,15] that the short thermomechanical responses are generated by two competing mechanisms, namely (a) stress generation, which arises largely from entropic forces exerted by contracting segments in the amorphous phase and to a lesser extent from the melting of ordered regions at appropriate temperatures, and (b) stress relaxation, which results primarily from crystallization or recrystallization, molecular disorientation and at least some viscoelastic flow, which may be preceded by network rupture leading to disentanglement and intermolecular slippage.

Stress relaxation as a result of crystallization has been explained as follows[23]. When part of a molecular chain is incorporated in a crystallite as a result of oriented crystallization, the average stress that it exerts at its end points is reduced. Also the distance traversed by the remaining amorphous units is reduced because of the greater distance taken by the crystalline units. Consequently, the retractive force exerted is diminished by the crystallization process. While crystallization results in elongation of the oriented system in the axial direction, melting results in contraction, and thus is a stress-generating mechanism.

It needs to be emphasized that these observations apply to an isothermal situation and for a short time interval as in the present case, and that the crystallization process can generate a residual stress field in the fibre (a) at longer times, which has been attributed to a different mechanism of crystallization that occurs at that stage[24], as explained below, and (b) after the heat treatment process has ended and as the sample is brought back from T_g to room temperature[25]. These latter stresses arise as a result of the difference in the coefficient of contraction between the crystals and the amorphous regions.

According to the model proposed by Kawai *et al.*[24] for oriented crystallization, the initial stage leads to loose, uncrystallized material remaining between the crystals as a result of structural reorganization, this being consistent

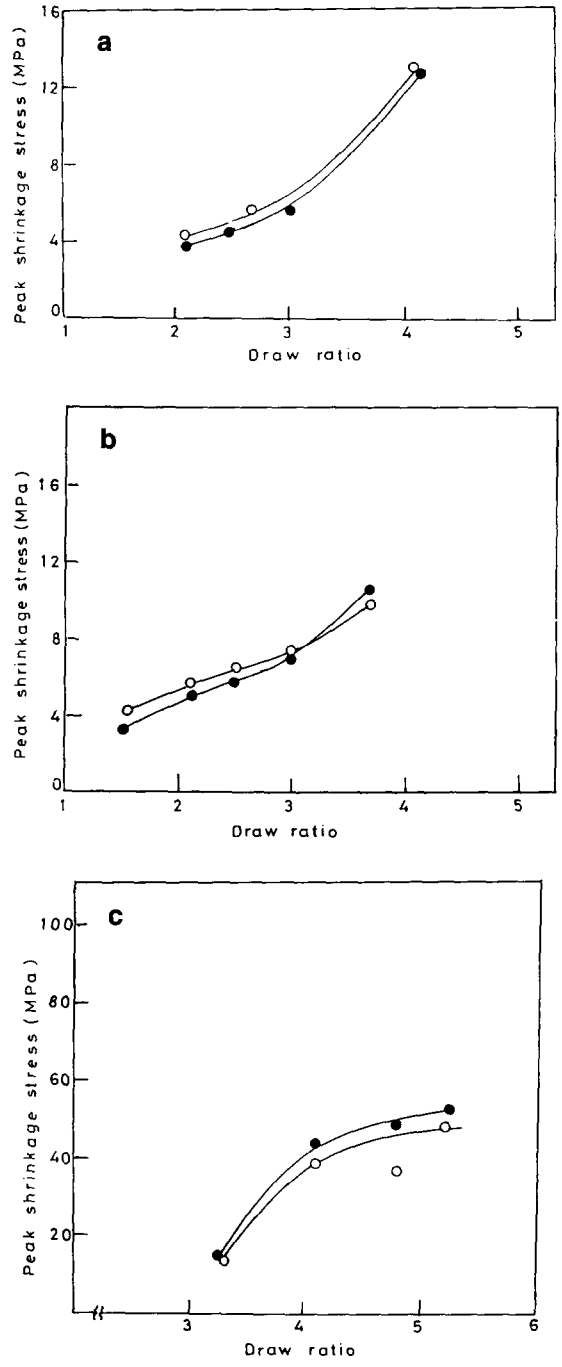

Figure 4 Peak shrinkage stress as a function of draw ratio at 100°C (○) and at 220°C (●): (a) film drawn in water; (b) film drawn in air; (c) POY drawn in air

with the proposal of Mandelkern[23] described earlier. This accounts for the decrease in stress. In the later stages of crystallization, as the crystals grow further, the link molecules between the crystals become more taut, according to Kawai *et al.*, thus increasing the stress.

It may be noted from a close examination of *Figures 1b* and *1c* that, when samples 1 to 4 are subjected to a heat treatment temperature of 220°C, the maximum in shrinkage stress is reached at much lower temperatures, which are close to T_g. This suggests that the forces of contraction of the oriented network become dominant around T_g. Since these forces represent the principal mechanism of stress generation, σ_{max} is not significantly different at 100 and 220°C.

(iii) Shrinkage stresses are significantly lower for the film-based samples than for those based on POY, as would be expected from the dependence of shrinkage stress on orientation and frozen-in axial stress, as discussed earlier.

(iv) The air-drawn and water-drawn samples show similar behaviour, thus indicating that the medium of drawing does not play a dominant role in the thermomechanical behaviour of the samples.

Structural dependence of thermomechanical behaviour

On the basis of the preceding discussion and the structural data presented in *Table 3*, the samples whose thermomechanical behaviour is presented in *Figures 1a* and *1b* may be subdivided into the following three categories.

(i) Samples having *very low X-ray crystallinity* and *very low molecular orientation*: Sample 1 and to a limited extent sample 2 belong to this category. When these samples are held at constant length at elevated temperature, the shrinkage stress builds up rather slowly to a relatively low σ_{max}. At 100°C, the stress relaxation is complete for sample 1 and rather small for sample 2. At 220°C, the stress relaxation is almost complete for both samples. Because of the low orientation, the crystallization kinetics are slow and the thermomechanical behaviour over the first 15 s or so is dominated by the oriented amorphous phase. Such behaviour is typical of an amorphous polymer with an oriented network. The stress generation in such cases may be attributed to entropic forces and the relaxation to disorientation, just as in the case of a rubber-like network.

(ii) Samples having *very low X-ray crystallinity* but *high molecular orientation*: Samples 3 and 4 belong to this category. When held at constant length at elevated temperature, the shrinkage stress rises rapidly in these samples. Such rapid development of stress is generally attributed to high amorphous orientation and, as shown in *Table 3*, the amorphous orientation factor for these samples is significantly higher than for samples 1 and 2.

Though the f_a values after heat treatment have not been measured for the present samples, such measurements have been made[26,27] on similar samples that were taut annealed while held at constant length in silicone oil at an elevated temperature for 3 min. The relevant data are given in *Table 4*. It is apparent that, even under constant-length conditions, amorphous disorientation can occur though the absolute value of birefringence does not show any significant change (*Table 3*). Thus amorphous disorientation and crystallization

Table 4 Effect of heat setting on amorphous orientation factor[26,27]

	Amorphous orientation factor, f_a		
		After heat treatment	
Sample	Control	100°C	220°C
LOY-based sample of draw ratio 4.1 (ref. 26)	0.582	0.519	0.433
Water-drawn film of draw ratio 4.16 (ref. 27)	0.71	0.637	0.377

Table 5 Boiling water shrinkage of heat-treated samples

	Boiling water shrinkage (%)		
		After heat treatment	
Sample No.[a]	Control	100°C	220°C
1	50	0	0
2	52	0	0
3	18	1	1
4	21	0	0
5	35	5.4	5
6	32	6.7	4

[a] As in *Table 2*

are the two major stress-relaxation mechanisms that become operational when the samples that have been studied are subjected to elevated temperatures. Some further comments on these mechanisms will be made later.

(iii) Samples having *significant X-ray crystallinity* and *high molecular orientation*: Samples 5 and 6 belong to this category. When these samples are heated at constant length, the shrinkage stress rises rapidly (*Figures 1a* and *1b*) owing to their amorphous orientation being high. However, unlike the remaining samples, the shrinkage stress that is generated at 100 and 220°C does not relax with time within the short time period studied, and a considerable amount of stress resides within the sample. Since boiling water shrinkage is a measure of residual stress, such measurements were made on samples heat treated at constant length for 12 s at 100 and 220°C and the results are summarized in *Table 5*. It is apparent that, compared with the other samples, samples 5 and 6 show significant shrinkage, signifying the presence of axial residual stress in these samples. However, as shown in *Table 5*, the boiling water shrinkage of samples 5 and 6 in the as-drawn (control) state is much greater than that after heat treatment. There are two likely reasons for this. The first relates to the morphological changes that occur on heat setting. It is possible that a crystalline structure with high continuity can develop and improve the stability of the sample despite a higher level of initial stresses that were introduced. The second possibility is that some residual stress dissipation may occur during the heat treatment itself. This would mean that the entropic forces of contraction that result in stress generation are attenuated by a stress-relaxation mechanism like crystallization during the initial rise of stress itself.

The stress-relaxation mechanisms

In the samples studied in the present investigation, amorphous disorientation and crystallization appear to be the principal stress-relaxation mechanisms. It has also been suggested that growing crystals can stabilize the oriented state with the possibility of a certain amount of locked-in residual stresses being frozen within the sample.

There is a need for further work in this area if a clear understanding of the stress-relaxation mechanisms, particularly the role of crystallization, during constant-length heating of oriented PET samples is to be gained. There are a number of contributions in this area that are relevant to the present study, three of which are as follows.

(i) The first set of contributions relates to the mechanism of crystallization in the solid state. Two possible mechanisms have been suggested. The first is through

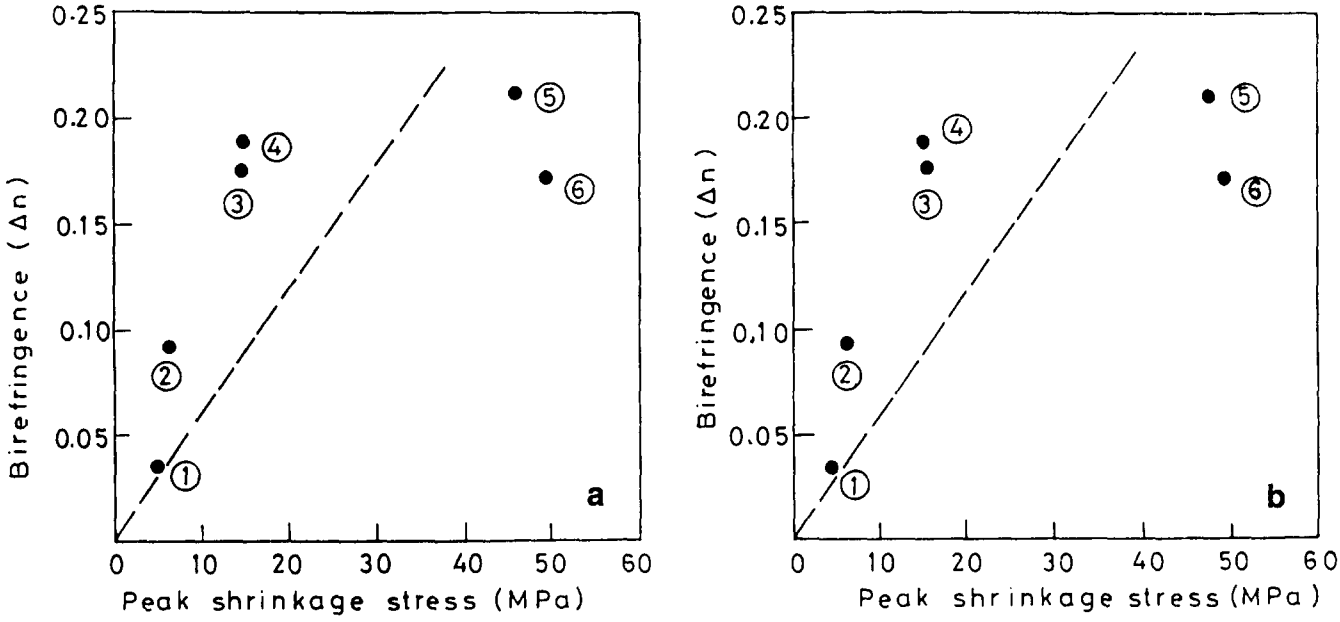

Figure 5 Plots of peak shrinkage stress vs. birefringence at (a) 100°C and (b) 220°C (sample numbers as in *Table 2*)

the melting of small, imperfect crystals followed by recrystallization into a new form[28,29], or by solid-state transformation in which molecules in the amorphous regions that are not in exact register can, with the aid of thermal energy, gain enough mobility to reduce their free energy by forming small crystals[30,31]. (ii) The second relates to the crystallization of POY under a fixed load at temperatures from 140 to 230°C at times up to 800 ms[32]. It was concluded from this study that, under low load and low temperature, three-stage crystallization occurs; while under high load and high temperature, crystallization occurs in two stages. (iii) The third contribution is due to Pakula and Fischer[33], who have pointed out that, for PET samples drawn at constant stress, a critical stress exists below which the samples draw slowly and remain near-amorphous, while above it the samples deform rapidly and crystallize during drawing.

In a separate study[16], the crystallization kinetics of samples 3 and 4 have been shown to be faster than those of samples 5 and 6. Also, since samples 3 and 4 have a distorted paracrystalline type of structure with very low X-ray crystallinity, structural reorganization in these samples is likely to occur by preferential crystallization of the oriented amorphous regions, while in samples 5 and 6, recrystallization around the existing crystallites is likely to be the dominant mechanism. The nature and the effect of different modes of structural reorganization on thermomechanical behaviour needs to be studied in greater detail.

Stress-optical characteristics

The values of σ_{max} for samples 1 to 6 measured at 100 and 220°C are plotted as functions of sample birefringence in *Figures 5a* and *5b* respectively. Though the statistical network theory is only likely to predict a linear behaviour for low degrees of orientation, broken lines have been drawn to give a stress-optical coefficient (*SOC*) $\Delta n/\sigma_{max}$ of $5.5 \times 10^{-9}\ m^2\ N^{-1}$, as these are helpful later in interpreting the results. This value of *SOC* has been found to be valid for a range of PET samples[8,34].

Since most of the samples are semicrystalline, a part of the measured birefringence is derived from the crystalline component of the sample. The shrinkage stress, however, is primarily related to the amorphous component. Hence, following Bhatt and Bell[35], it was considered instructive to plot σ_{max} as a function of $\Delta n_a/(1-\beta)$ for the data at 100 and 220°C. Since these plots are similar to *Figures 5a* and *5b*, they are not included.

The following observations are noteworthy:

(i) Sample 1 with very low crystallinity and low orientation lies on the broken line, suggesting that its thermomechanical behaviour can be described by the statistical theory of rubber elasticity, a conclusion derived earlier on the basis of other experimental evidence.

(ii) Samples 2, 3 and 4 lie to the left of the broken line, indicating that the stress generated is less than that warranted by rubber elasticity theory. As pointed out earlier, the stress-relaxation mechanisms might be acting concurrently and thus the stress generated in these samples is reduced.

(iii) Samples 5 and 6 lie to the right of the broken line, indicating that the stress generated is much higher. These samples have significant crystallinity and their thermomechanical response can therefore not be analysed within the framework of the simple theory of rubber elasticity.

CONCLUSIONS

In this paper the thermomechanical behaviour of axially oriented PET fibres and films prepared by varying the spinning speed in the case of fibres and the speed, temperature, medium and extent of drawing for both fibres and films were studied. The dependence of shrinkage stress on sample draw ratio and on temperature has also been studied. Samples prepared at low speeds developed low shrinkage stress, which decayed with time, while those prepared at higher speeds developed high stress, which showed little relaxation with time. On the basis of the structural data presented, it is concluded that in all samples the stress is generated around T_g as the

extended molecules in the amorphous regions of the fibre tend to a more coiled conformation because of entropic considerations. The stress relaxation is mainly due to disorientation of the molecules in the amorphous regions or as a result of crystallization of the samples with very low crystallinity.

REFERENCES

1 Trznadel, M. and Kryszewski, M. *J. Macromol. Sci., Rev. Macromol. Chem. Phys.* (*C*) 1992, **32**, 259
2 Trznadel, M. and Kryszewski, M. *Polymer* 1988, **29**, 418
3 Pakula, T. and Trznadel, M. *Polymer* 1985, **26**, 1011
4 Trznadel, M., Pakula, T. and Kryszewski, M. *Polymer* 1985, **26**, 1019
5 Trznadel, M. *J. Macromol. Sci., Phys.* (*B*) 1989, **28**, 285
6 Dennis, L. A. and Buchanan, D. R. *Text. Res. J.* 1987, **57**, 625
7 Perena, J. M., Duckett, R. A. and Ward, I. M. *J. Appl. Polym. Sci.* 1980, **25**, 1381
8 Pinnock, P. R. and Ward, I. M. *Trans. Faraday Soc.* 1966, **62**, 1308
9 Capaccio, G. and Ward, I. M. *Colloid Polym. Sci.* 1986, **260**, 40
10 Long, S. D. and Ward, I. M. *J. Appl. Polym. Sci.* 1991, **42**, 1921
11 Heuvel, H. M., Lucas, L. J., Van Den Heuvel, C. J. M. and Weijer, A. P. J. *J. Appl. Polym. Sci.* 1992, **45**, 1649
12 Hearle, J. W. S. and Mukhopadhyay, S. K. 'Resumé of Papers' 27th Joint Technol. Conf., Northern India Textile Research Association, Feb. 1986, IIT, Delhi
13 Desai, P. and Abhiraman, A. S. *J. Polym. Sci., Polym. Phys. Edn.* 1985, **23**, 653
14 Batra, S. K. *J. Macromol. Sci., Phys.* (*B*) 1976, **12**, 405
15 Buchanan, D. R. in 'Advances in Fibre Science' (Ed. S. K. Mukhopadhyay), Textile Institute, Manchester, 1992, pp. 87–113
16 Gupta, V. B., Radhakrishnan, J. and Sett, S. K. *Polymer* 1993, **34**, 3814
17 Radhakrishnan, J. and Gupta, V. B. *J. Macromol. Sci., Phys.* (*B*) 1993, **32**, 243
18 Daubney, R. P., Bunn, C. W. and Brown, C. J. *Proc. R. Soc.* (*A*) 1954, **226**, 531
19 Gupta, V. B., Ramesh, C. and Gupta, A. K. *J. Appl. Polym. Sci.* 1984, **29**, 3115
20 Stein, R. S. and Norris, F. H. *J. Polym. Sci.* 1956, **21**, 381
21 Dumbleton, J. H. *J. Polym. Sci.* (*A*) 1968, **26**, 795
22 Ziabicki, A. 'Fundamentals of Fibre Formation', Wiley, London, 1976, p. 454
23 Mandelkern, L. 'Crystallisation of Polymers', McGraw-Hill, New York, 1964, p. 167
24 Kawai, T., Iguchi, M. and Tonami, H. *Kolloid Z. Polym.* 1967, **221**, 28
25 Sweet, G. E. and Bell, J. P. *J. Polym. Sci., Polym. Phys. Edn.* 1978, **16**, 2057
26 Jain, A. K. and Gupta, V. B. *J. Macromol. Sci., Phys.* (*B*) 1990, **29**, 49
27 Sett, S. K. PhD Thesis, Indian Institute of Technology, Delhi, 1989
28 Groeninckx, G., Reynaers, H., Berghmans, H. and Smets, G. *J. Polym. Sci., Polym. Phys. Edn.* 1980, **18**, 1311
29 Groeninckx, G. and Reynaers, H. *J. Polym. Sci., Polym. Phys. Edn.* 1980, **18**, 1325
30 Fakirov, S., Fischer, E. W., Hoffman, R. and Schmidt, G. F. *Polymer* 1977, **18**, 1121
31 Wu, W., Riekel, C. and Zachmann, H. C. *Polym. Commun.* 1984, **25**, 76
32 Hristov, H. A. and Schultz, J. M. *Polymer* 1988, **29**, 1214
33 Pakula, T. and Fischer, E. W. *J. Polym. Sci., Polym. Phys. Edn.* 1981, **19**, 1705
34 Garg, S. K. *J. Appl. Polym. Sci.* 1982, **27**, 2857
35 Bhatt, G. M. and Bell, J. P. *J. Polym. Sci., Polym. Phys. Edn.* 1976, **14**, 575